

# Modeling of Open, Closed, and Open-Inactivated States of the hERG1 Channel: Structural Mechanisms of the State-Dependent Drug Binding

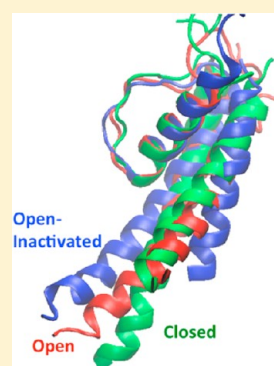
Serdar Durdagi,<sup>†</sup> Sumukh Deshpande,<sup>†</sup> Henry J Duff,<sup>\*,‡</sup> and Sergei Y. Noskov<sup>\*,†</sup>

<sup>†</sup>Institute for Biocomplexity and Informatics, Department of Biological Sciences, University of Calgary, Alberta, Canada

<sup>‡</sup>Libin Cardiovascular Institute of Alberta, University of Calgary, Calgary, Alberta, Canada

## S Supporting Information

**ABSTRACT:** The human ether-a-go-go related gene 1 (hERG1) K ion channel is a key element for the rapid component of the delayed rectified potassium current in cardiac myocytes. Since there are no crystal structures for hERG channels, creation and validation of its reliable atomistic models have been key targets in molecular cardiology for the past decade. In this study, we developed and vigorously validated models for open, closed, and open-inactivated states of hERG1 using a multistep protocol. The conserved elements were derived using multiple-template homology modeling utilizing available structures for Kv1.2, Kv1.2/2.1 chimera, and KcsA channels. Then missing elements were modeled with the ROSETTA *De Novo* protein-designing suite and further refined with all-atom molecular dynamics simulations. The final ensemble of models was evaluated for consistency to the reported experimental data from biochemical, biophysical, and electrophysiological studies. The closed state models were cross-validated against available experimental data on toxin footprinting with protein–protein docking using hERG state-selective toxin BeKm-1. Poisson–Boltzmann calculations were performed to determine gating charge and compare it to electrophysiological measurements. The validated structures offered us a unique chance to assess molecular mechanisms of state-dependent drug binding in three different states of the channel.



## INTRODUCTION

Biological ion channels are membrane-inserted proteins regulating the movement of ions (e.g., Na<sup>+</sup>, K<sup>+</sup>, Ca<sup>2+</sup>, Cl<sup>−</sup>) across the hydrophobic interior of the cell membrane by providing a water-filled pathway. Controlled opening and closing of ion channels in cardiac myocytes results in electrical excitations and relaxations, an integral mechanism for normal functioning of the heart. A unique component of this mechanism is the presence of potassium (K) channels, which shape signaling by selective permeation of K<sup>+</sup> in response to electrical or chemical signal. Abnormalities resulting from inherited mutations and/or pharmacological blockade of voltage- and ligand-gated K channels may potentially lead to prolongation of the action potential and are considered to be pro-arrhythmic.<sup>1</sup> One of the K channels, human ether-a-go-go related gene 1 (hERG1), is particularly infamous for its ability for promiscuous intracavitary binding of many organic molecules associated with drug-induced arrhythmias in humans.

Similar to other voltage-gated ion channels hERG1 displays a distinct multistate conformational dynamics in response to changes in membrane potential. A nonconductive (closed) state of the channel is stabilized at negative membrane potentials (below −80 mV). Depolarization of the membrane to more positive values (up to −60 mV) leads to channel opening (activation) and allows outward potassium current. A landmark of the hERG1 channel functional dynamics is rapid C-type inactivation. C-type inactivation occurs while the activation gate

may still be open, but local conformational changes in the pore domain result in loss of potassium permeation. C-type inactivation in hERGs is sensitive to a multitude of factors such as external cation concentrations, local mutations in the pore domain (i.e., S631A and S620T), and the presence of drugs.<sup>2</sup> During repolarization, recovery from C-type inactivation generates a large repolarizing tail current, which apposes any spurious depolarizing forces. This may explain why the hERG current is considered to have antiarrhythmic properties. Despite years of functional studies, structural understanding of gating transitions in hERG is yet to be developed. Establishing a link between channel and blocker structures and identification of specific interactions governing high-affinity blockade of cardiac K channels pose major challenges to rational design of antiarrhythmic agents as well as for ensuring safe drug development.

The starting point for molecular-level understanding of drug interactions with hERG1 is identification of key players in the high-affinity, high-specificity drug binding as well as structural mechanisms underlying channel activation/inactivation. Various experimental techniques were employed for this purpose, e.g., structures of ligand-bound complexes are determined by X-ray crystallography and NMR, binding energies from rate constants, and specific pairs of residues involved in binding

Received: July 28, 2012

Published: September 18, 2012

from site-directed mutagenesis studies. While experiments can provide a fairly complete description of a single protein–ligand complex, they are too labor intensive in ligand screening projects. Therefore, theoretical models can assist the successful utilization of ion channels dynamics found in humans and hERGs in particular. We recently developed atomistic protein models of pore and voltage sensing trans membrane (TM) domains of the hERG1 potassium ion channel representing the channel in open state conformation.<sup>3</sup> In this model, KvAP, Kv1.2, and Kv1.2-Kv2.1 chimera and KcsA channels were used as template and the missing parts are modeled de novo.

In the current study, together with the refinement of open state S1–S6 TM hERG1 models (i.e., Kv1.2), two conformational states (i.e., closed and open-inactivated) were modeled and refined against available experimental data (see Methods section for details). The closed state for the hERG1 S1–S6 TM domain was modeled based on the Kv1.2 closed state structure published by Yarov–Yarovoy et al.<sup>4</sup> Publication of the first potassium channel in its C-type inactivated conformation<sup>5,6</sup> puts us into a position to develop such a model for hERG1. Accordingly, the structure for the open-inactivated state was modeled using the available crystal structure for the C-type inactivated KcsA channel (pdb, 3F5W). In all of the modeling, we used the developed and experimentally validated hERG1 sequence alignment (Supporting Information, Figure S1) from our previous publications.<sup>3</sup>

It has been shown that pore domains for all of the crystallized K channels display high structural similarity for a given conformational state with rmsd values for the backbone atoms below 2 Å. The variation in the amino acid residues from channel to channel led to the diversity of the voltage-dependent gating mechanism, channel conductance, and toxin-binding properties, therefore allowing for a robust testing of the developed models. Taken together, the different approaches used in our work (ROSETTA protein modeling, domain docking, conventional homology modeling, and all-atom MD simulations) are striving to provide deeper insight into our understanding of K-channel structure and its conformational dynamics and state-dependent modulation by small organic molecules, an integrative approach for cardio-toxicity assessment, as well as to contribute to development of new strategies for a proactive approach to the design of drugs targeting the hERG1 channel.

## METHODS

**Combined De Novo/Homology Protein Modeling.** To perform homology modeling for parts of the structure conserved among K channels with known crystal structures, initially target-template sequence alignment has been performed by the ClustalW algorithm<sup>7</sup> which gives ~30% sequence similarity to Kv1.2 and KcsA sequences (see Supporting Information Figure S1). Homology models were produced by the Comparative Modeling module in ROSETTA<sup>8–10</sup> to produce reasonably good models with ~3–4 Å backbone C<sub>α</sub> RMSD. Since the pore domain (PD) contains an unusually long S5-Pore linker or turret which forms a 8–12-residue helix above the selectivity filter, de novo modeling of the linker and missing parts in the model was performed by Loop Modeling<sup>11,12</sup> in ROSETTA. Five steps are used in the protein modeling: (i) sequence alignment for generation of alignment based on one or more template structures, (ii) threading for generation of initial models based on template structure by copying coordinates over the aligned regions, (iii)

loop modeling for rebuilding the missing parts using de novo modeling, (iv) selection of models based on reported experimental data from biochemical, biophysical, and electrophysiological studies, and (v) refinement using all-atom molecular dynamics (MD) simulations with reported constraints for the interatomic distances of the salt-bridge interaction pair obtained from electrophysiology and mutagenesis experiments performed on hERG channels. (see Supporting Information Figure S2 for more details).

The previously published sequence alignment was used<sup>13</sup> for modeling the hERG1 channel in open, closed, and inactivated states. Open and closed state S1–S6 TM models are modeled based on the refined Kv1.2 model which is derived from the Kv1.2 crystal structure (PDB ID 2A79) and Kv1.2 closed state protein model, respectively.<sup>10,14</sup> Open state Kv1.2, closed Kv1.2,<sup>15</sup> and open-inactivated KcsA PD (PDB ID 3F5W) from *Mus musculus* were used as template structures. Intracellular (IC) and extracellular (EC) domains such as antibody light and heavy chains from the available PDB coordinate files were trimmed off for generating initial incomplete models of hERG1 in S1–S6 open and closed states and S5S6 in the open-inactivated state.

Loop modeling is one of the key components in homology modeling as it participates in many biological events and functional aspects such as ligand–receptor interactions. However, due to their flexible/dynamic nature, it is often very difficult to predict their native conformations. For optimal loop prediction in hERG1, fragment-based loop modeling of ROSETTA was implemented.<sup>11,12</sup> It performs a fragment-based conformational search which uses cyclic coordinate descent (CCD) and kinematic loop closure (KLC) algorithms for inserting 3- and 9-residue-long fragments of protein structures from the PDB fragment library, and secondary structure prediction was generated by PSIPRED.<sup>16</sup> Over 20 000 models for open, closed, and open-inactivated states were generated using loop modeling. Models with a 8–12-residue helix located in the outer mouth of the selectivity filter were selected for further analysis with the Molsoft ICM program.<sup>17</sup> The stable models complying with published experimental constraints were used for subsequent all-atom MD simulations.

**Incorporation of Experimental Constraint into Model Selection and Refinement.** The genuine challenge in hERG1 TM modeling with all the conformational states is to generate an appropriate model satisfying all of the conformational constraints of open, closed, and open-inactivated states reported in electrophysiology experiments. In the current modeling study available experimental constraints (i.e., known salt-bridge contacts between positively charged residues at the S4 helix and negatively charged residues at S1–S3)<sup>18,19</sup> have been implemented during de novo modeling with ROSETTA. Most of the homology models of hERG1 to date failed to model the outer mouth region, rendering studies of the toxin interactions to the outer mouth in the closed state and antiarrhythmic drug binding in open and inactivated states impossible. In this study, modeling of flexible linkers responsible for toxin binding offers a route for elucidation of the possible topology for hERG–toxin interactions as well as narrows down the number of models selected for all-atom MD simulations.<sup>20</sup>

**Molecular Docking.** Protein–ligand and protein–protein interactions were examined by Schrodinger's Glide/Induced Fit Docking (IFD) and High Ambiguity Driven Docking (HADDOCK) protein–protein docking programs, respec-

tively. Geometry optimization calculations for ligands were performed with the Schrodinger's Maestro module using Polak–Ribiere conjugate gradient (PRCG) minimization (with 0.0001 kJ Å<sup>-1</sup> mol<sup>-1</sup> convergence criteria).<sup>21</sup> Protonation states of ligands and residues were tested using LigPrep and Protein Preparation modules with the Schrodinger package at pH 7. The Glide-XP (extra precision) (v5.0)<sup>22</sup> combined with IFD has been used for docking calculations.<sup>22,23</sup> IFD uses the Glide docking program to account for ligand flexibility and the Prime<sup>24</sup> algorithm to account for flexibility of the receptor. Schrodinger's IFD protocol model uses the following steps (the description that follows is from the IFD user manual). (i) Constrained minimization of the receptor with an rmsd cutoff of 0.18 Å. (ii) Initial Glide docking of each ligand using a soft potential (0.5 van der Waals radii scaling of nonpolar atoms of ligands and receptor using a partial charge cutoff of 0.15). (iii) Derived docking poses were refined using the Prime module of Schrodinger. Residues within 5.0 Å of the ligand poses were minimized in order to form suitable conformations of poses at the active site of the receptor. (iv) Glide redocking of each protein–ligand complex.

A toxin (BeKm-1, pdb 1J5J) was docked to the initial closed state models using HADDOCK (v. 2.0)<sup>25</sup> for their validations. This toxin is known to target the closed state of the hERG1 channel. The protein–protein docking protocol consists of rigid body energy minimization, torsion angle space refinement, and refinement in explicit solvent. After each of these stages, all of the complexes are scored and ranked. The score is the weighted sum of van der Waals, electrostatic, desolvation, and restraint violation energies.

**MD Simulations.** All-atom MD simulations were carried out for the selected models using CHARMM (v. c36a2). All simulations were carried out at 323 K and 1 atm using the periodic boundary conditions (PBC) of NPT ensemble. Similar to previous MD simulations<sup>9</sup> of K channels, the particle mesh Ewald (PME) algorithm was used for electrostatic interactions. K ions at the selectivity filter were used as the occupation of ions at the S0:S2:S4 positions according to the previous studies.<sup>9</sup> Each model was embedded into the DPPC membrane bilayer using the CHARMM-GUI membrane builder protocol.<sup>26,27</sup> The simulation box contained 1 protein, 264 DPPC molecules (corresponding number of lipid molecules are 132 for simulations that limited to PD), 3 K<sup>+</sup> ions, pore water molecules in the intracellular cavity, solvated by 0.15 M KCl aqueous salt solution. Total atoms in the simulation systems were ca. 90 000 and 150 000 atoms for S5S6 and S1–S6 TM models, respectively. Structures were minimized and equilibrated with gradually decreasing harmonic constraints (i.e., started with 10.0 and 5.0 kcal mol<sup>-1</sup> Å<sup>-2</sup> for backbone and side chains, respectively, and gradually decreased to 0.5 and 0.1 kcal mol<sup>-1</sup> Å<sup>-2</sup>) for 2 ns and then subjected to a 7.5 ns production run.

**Gating Charge Calculations.** Trajectories from the last 5 ns of MD simulations of closed and open state models were used for gating charge calculations. Corresponding frames from open and closed state models were aligned before the calculations. These calculations are performed with the APBSmem program.<sup>28</sup> A cubic grid with dimensions of 97 Å × 97 Å × 97 Å with a focusing scheme was used. Salt concentration was set to 0.15 M (symmetric monovalent salt concentration) mimicking physiological conditions with 2 Å probe radii being used for the bathing solution. Dielectric constants for the membrane and water are set to 4 and 80,

respectively (dielectric constant for head groups of membrane is also set to 80). The protein's dielectric constant was set to 4 according to the scheme used by Jogini and Roux.<sup>29</sup> The Poisson–Boltzmann (PB) equation (eq 1) for the one-to-one electrolyte solution is used for gating charges. Since the nonlinear form of the PB equation (NPBE) has better accuracy and range validity compared to the linear form of the PB equation (LPBE);<sup>30</sup> NPBE is solved using focused boundary conditions at 315 K. The membrane potential of the inner bath is set to vary from +100 to -100 mV

$$-\nabla \cdot [\epsilon(\vec{r}) \nabla \phi(\vec{r})] + \bar{\kappa}^2(\vec{r}) \sinh[\phi(\vec{r})] = \frac{e}{k_B T} 4\pi \rho(\vec{r}) \quad (1)$$

where  $\epsilon$  is the dielectric constant,  $\rho$  is the density of charge within the protein moiety,  $\kappa^2$  is the Debye–Huckel screening parameter for ionic shielding, and  $\phi$  is the reduced electrostatic potential.

## RESULTS

Selected hERG1 models representing open, closed, and inactivated states are subjected to 7.5 ns MD simulations (after running 2 ns equilibration) in the explicit membrane bilayer to evaluate stabilities and further refine the structure of the membrane-inserted domains in the presence of solvent and lipids. Subsequently, validation studies for the selected protein models have been performed. The Protein reports module of Schrodinger used for checking the Ramachandran plots, steric clashes, bond length deviations, bond angle deviations, backbone dihedrals, side-chain dihedrals, G factors, peptide planarity, improper torsions, C<sub>α</sub> stereochemistry, and missing atoms for the derived hERG1 models (Supporting Information, Figures S3 and S4). These reports helped us to filter out models that do not fit a range of various structural properties (which are calculated as average structural values of the protein library at *Protein reports*) of protein models. Below, we will summarize results of the molecular modeling and drug-binding data.

**i. Open State Models.** The S5-pore helix linker of hERG1 includes a 8–12-residue-long amphipathic  $\alpha$ -helix located at the outer mouth of the selectivity filter.<sup>1</sup> Out of 20 000 models from the ROSETTA-TM loop predictions protocol, only structures with the short helix in the S5-pore linker were selected. These models were further constrained using reported salt bridges for intra- and inter-residual contacts that were derived from electrophysiology studies on the hERG1 K channel in voltage sensing domains (VSD).<sup>19,31–35</sup> These contacts for 18 open state homology models are listed in Table S1 in the Supporting Information.

Backbone RMSD and alignment scores of homology models to Kv1.2 template structure was calculated and listed in Table S2 in the Supporting Information. Backbone RMSD is the average distance between the backbone atoms of superimposed proteins. Alignment score measures the 'matching score' of a given pair of amino acid residues obtained from superimposition of the given homology model and the template structure. The reported backbone rmsd plateaued at ~5–6 Å for some of the open state models. These high values are defined by the presence of flexible elements (linkers, elongated turret region in the S5-pore linker) in the hERG1 channel. These structural elements are not present in the Kv1.2 crystal structure, which generates a slight deviation from the template structure. The backbone RMSDs for the conserved elements of



the structure plateaued at 3–4 Å (see Supporting Information Table S2).

The set of developed models was ranked for the ability to reproduce binding data for well-studied hERG1 blockers. We chose to study high-, moderate-, and low-affinity open channel blockers (i.e., dofetilide, KN93, haloperidol, E4031, and carvedilol). The selected molecules were docked with the induced fit docking (IFD) protocol at the central cavity of the open state models. Dofetilide ( $pIC_{50}$ , 8.02) and E4031 ( $pIC_{50}$ , 7.74) were used as representative of high-affinity hERG blockers followed by KN93 ( $pIC_{50}$ , 6.96) as representative of moderate blockers. Haloperidol ( $pIC_{50}$ , 5.72) and carvedilol ( $pIC_{50}$ , 4.98) were considered as weak blockers.<sup>37</sup> The aim of performing IFD for diverse binding affinity blockers is to filter out the derived model that is not able to discriminate low/high-affinity drug binding at the central cavity of channel. The estimated free energy of binding of the drug is calculated for every conformational pose. IFD scores that are calculated for all open state models were listed in Table 1.

Out of 18 models developed for the channel, only eight models are capable of successful discrimination between high- and low-affinity blockers. A few models (i.e., 81, 514, 732) displayed clear discrimination between high- and moderate/low-affinity blockers with IFD scores (Table 1). Model 81 has high (absolute values) IFD and Glide extra precision (XP) scores for high-affinity blockers dofetilide and E4031. These scores are low for the weak blockers haloperidol and carvedilol (Table 1). A similar trend was also observed for models 732 and 514 (Table 1). MD simulations (7.5 ns) have been performed for these three models in order to refine and test their stabilities and for further analyses. The average root mean square fluctuations (RMSF) values of the channel backbone atoms relative to the initial structure were used to judge the stability of the models. The representative 3D structure for an open state model (732) of hERG1 is shown in Figure 1.

RMSF per residue are shown for the developed open, closed, and inactivated state models in Figure 2. The selectivity filter and PD are very stable throughout the simulations. These regions have an RMSF of ca. 1.5–2.0 Å. The most flexible regions of the channel as expected are S5-pore linker and EC and IC linkers (RMSF < 4.0 Å). This range of fluctuations for the flexible domains of the structure is not surprising. Similar numbers for the dynamics of the flexible parts of VSD are reported in previous Kv channel studies.<sup>38</sup> Of particular importance for the models is the dynamics of negatively charged side chains from S1–S3 helices and their salt bridging to basic residues at S4 (see Discussion). These salt-bridge interactions at the VSD of an open state conformation (model 732) of hERG1 is shown in Figure 3. A change of salt-bridge distances during MD simulations has been also investigated (Figure S5, Supporting Information).

**ii. Open-Inactivated State Models.** The open-inactivated state models were constructed using ROSETTA for PD of hERG1 using a similar protocol mentioned above. There is an apparent correlation between the binding affinity for many hERG1 blockers and the conformational state of the channel suggesting stabilization of the blocker in the channel's binding site by conformational rearrangements during inactivation.<sup>39</sup> This suggests a possibility for state-dependent drug binding and hERG-related current modulation, which necessitates development of drugs for cardiac diseases. The mechanism by which state-dependent drug amplifies blockade by C-type inactivation process remains to be poorly understood. Accordingly, an

Table 1. Docking Results of Open State Homology Models from Glide/IFD<sup>a</sup>

model no.	dofetilide ( $pIC_{50}$ , 8.02)		KN93 ( $pIC_{50}$ , 6.96)		haloperidol ( $pIC_{50}$ , 5.72)		E4031 ( $pIC_{50}$ , 7.74)		carvedilol ( $pIC_{50}$ , 4.98)	
	IFD score (kcal/mol)	Glide XP score (kcal/mol)	IFD score (kcal/mol)	Glide XP score (kcal/mol)	IFD score (kcal/mol)	Glide XP score (kcal/mol)	IFD score (kcal/mol)	Glide XP score (kcal/mol)	IFD score (kcal/mol)	Glide XP score (kcal/mol)
59	-1567.57	-10.33	-1561.73	-10.17	-1553.42	-8.17	-1563.87	-10.03	-1560.76	-10.48
81	-1545.77	-8.39	-1541.14	-7.96	-1538.34	-5.55	-1547.21	-10.16	-1537.74	-6.32
242	-1421.70	-7.92	-1416.48	-7.96	-1413.77	-7.41	-1417.46	-6.71	-1415.87	-8.48
466	-1475.53	-10.56	-1473.23	-9.57	-1471.31	-8.66	-1469.67	-6.42	-1475.05	-10.54
468	-1474.30	-6.84	-1472.79	-7.29	-1470.38	-7.08	-1474.81	-7.47	-1472.15	-8.43
501	-1525.65	-8.01	-1522.46	-9.72	-1518.93	-8.14	-1525.42	-8.26	-1522.72	-8.62
514	-1574.18	-9.43	-1573.28	-8.08	-1566.28	-5.63	-1572.91	-10.04	-1569.66	-6.87
732	-1217.41	-11.36	-1210.89	-10.29	-1208.37	-8.05	-1219.37	-12.61	-1208.94	-8.29

<sup>a</sup>The rest of the derived open state nonrefined models (10 models) could not derive successful docking poses.

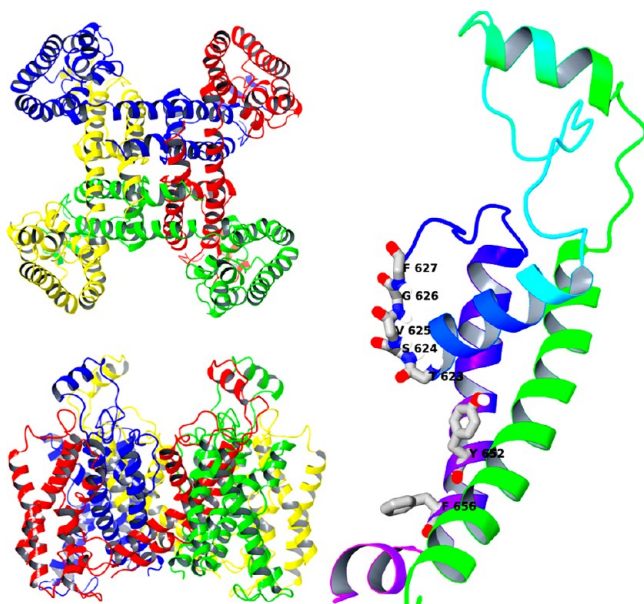


**Figure 1.** Representation of open state model 732 after MD simulations. (Left-top) Top view from EC; (left-bottom) side view; (right) selectivity filter and essential amino acids at the central cavity Y652 and F656 at PD for hERG channel blockers (for clarity, only one chain of the channel has been shown).

accurate understanding of the molecular basis for the blockade of the hERG channel is critical for design of safe drugs with a capacity to target a specific conformational state of the channel. The selected models were tested for their ability to bind hERG1 state-selective blockers. For this aim, two state-selective hERG1 blockers haloperidol and changrolin, which are known as open-inactivated state binders, docked at the EC domain of the channels using the Glide/IFD program.<sup>23</sup> Changrolin inhibits the hERG1 channel in a concentration-dependent and reversible manner. The maximal block of the channel is observed in the inactivated state with no further development of open channel blockade.<sup>40</sup> Chen et al.<sup>40</sup> found that channel inhibition by changrolin is voltage dependent. Inhibition increased at positive membrane potentials, and its association with a hyperpolarization shift in the voltage dependence of activation is observed.<sup>40</sup> These results show that changrolin blocks the channel in open and inactivated states, but favorable binding occurs at the inactivated state.

Haloperidol also displays preferential binding to an inactivated state of the channel.<sup>37</sup> Suessbrich et al.<sup>37</sup> reported voltage dependence of haloperidol blockade of hERG1. They concluded that since haloperidol increased the degree and rate of the hERG1 inactivation, the drug may preferentially target the open-inactivated state of the channel.<sup>37</sup> In the same study, a mutant channel (hERG1 S631A) and wild-type channels were compared for their inhibition by haloperidol. It was found that haloperidol blockade of the S631A mutant with altered C-type inactivation is about 4-fold weaker than for hERG1 wild-type channel.<sup>37</sup> The increased inactivation of hERG1 S631A mutant channels at such potentials corresponded to an increased haloperidol binding affinity against target, supporting the hypothesis that the inactivated state of the channel favors haloperidol binding.<sup>37</sup>

Thus, these two state-selective hERG1 blockers are used for the validation tests for derived selected open-inactivated state models. Although these two ligands have similar binding

affinities at the hERG1, the haloperidol-binding affinity (i.e.,  $pIC_{50}$ ) is slightly higher than changrolin ( $pIC_{50}$ , 5.72 and 4.74, respectively). Since experimental findings suggest S631 as a key residue for the haloperidol binding at the hERG1, models that display binding contacts with this residue are considered as another validation method for the constructed models. From the results shown in Table 2, models 1020 and 1979 are selected for further refinement tests. Model 1020 has been selected for further refinement because of its high (absolute) IFD and Glide XP docking scores. Furthermore, in this model haloperidol forms a hydrogen-bond interaction with S631 in accord with experimental data<sup>39</sup> (Supporting Information, Figure S6). Hydrogen bonding between haloperidol and S631 residue has been also observed at model 1979. This model also has the highest Glide XP docking score. Selected models are merged with the explicit membrane environment and prepared for all-atom MD simulations for testing their stabilities. For each model, 7.5 ns simulations have been performed by the CHARMM MD simulation program.

rmsd scan along the MD trajectory for an equilibrated ROSETTA-Membrane hERG1 open-inactivated state model (1020) has been shown in Figure 2 (ii). The maximum fluctuation ( $\sim 4.0$ – $4.5$  Å) is observed at the S5-pore linker region. The other domains of the channel are very stable throughout the simulation with an average RMSF value of  $\sim 1.5$ – $2.5$  Å. A representative model for an open-inactivated state (1020) and locations of aromatic amino acid residues at the intracellular cavity (i.e., F656, Y652) together with backbone selectivity filter residues is shown in Figure 4.

**iii. Closed State Models.** Closed state models were constructed and selected using the above-mentioned protocol. These models are validated by state-selective toxin binding analysis. BeKm-1 is a peptide toxin with known NMR structure, and its high-affinity hERG1 blockade is well known.<sup>20</sup> BeKm-1 toxin binds selectively to the closed state hERG1 target. While opening of the channel leads to weakening of toxin binding, channel inactivation causes unbinding of the toxin.<sup>20</sup> From the study performed by Tseng et al.,<sup>20</sup> a mutant cycle analysis together with molecular modeling was performed for identifying specific residues on the hERG1 outer mouth region involved in BeKm-1 interaction. The coupling energy between the toxin and the channel residues was used as an indicator for quantifying the interactions between the toxin and the channel. Residues within 4 Å of the toxin and channel display coupling energies  $> 1$  kcal/mol, which shows high-impact residues on the channel and toxin. These results showed that BeKm-1 binds to the channel in closed state and unbinds upon membrane depolarization when the channel makes a conformational transition from closed to open and then to the inactivated state.<sup>20</sup> The toxin was docked to the outer mouth of the selectivity filter using the HADDOCK protein/protein docking program<sup>25</sup> in our study. Peptide toxin footprinting data obtained from Tseng et al.<sup>20</sup> suggest that K18 and R20 of the toxin interact with Q592 and S631 residues on hERG1 closed state, respectively. Results from docking (Table S3, Supporting Information) show that only two models (i.e., 634 and 851) satisfied these two experimentally identified interactions (S631/K18 and Q592/R20). Together with S631/K18 and Q592/R20 interactions, model 851 also covers N633/K18, N573/S19, D591/R20, Q592/D4, and Y597/Y11 interactions (Supporting Information, Figure S7). These interactions are observed for N629/K18, G628/K18, and G590/R20 at model 634 that are high and substantial impact

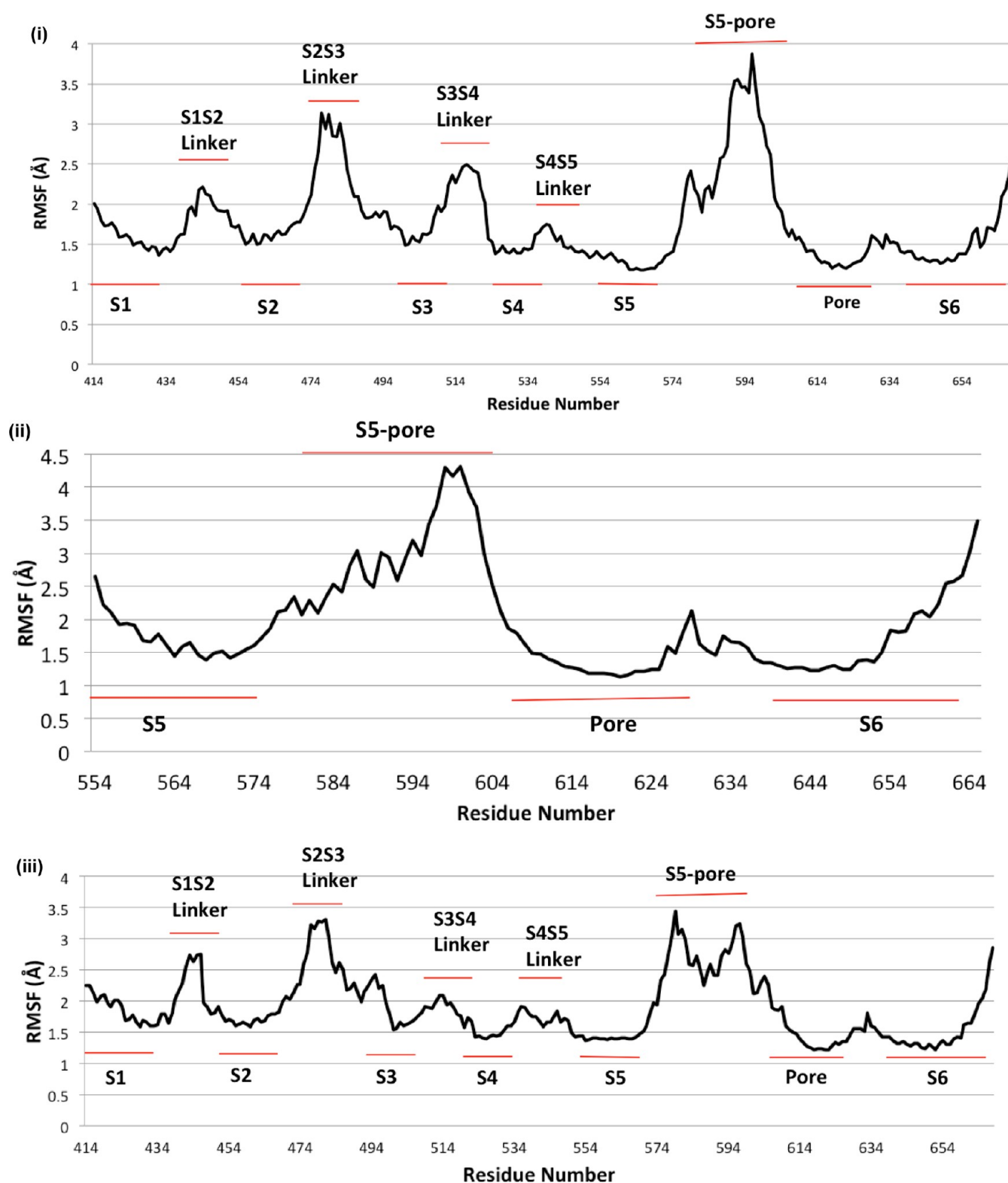


**Figure 2.** rmsd scans along MD trajectory for equilibrated ROSETTA-Membrane hERG1: (i) open state (model 732); (ii) open-inactivated state (model 1020); (iii) closed state (model 851). rms fluctuations (RMSF) for the pore domain and helical elements are around 1.5–2 Å, whereas most flexible elements (EC and IC linkers) display larger fluctuations of up to 4 Å from the average structure.

residues on hERG1 and BeKm-1 (Table S3, Supporting Information). The toxin footprinting suggests that bound toxin may interact simultaneously with the amphipathic helix in the S5P-linker and the pore residues at the outer mouth of the selectivity filter. The HADDOCK docking resulted in a

channel/toxin complex with sets of interacting partners similar to the one published by Tseng et al.<sup>20</sup> (i.e., conserved interactions of K18/S631, R20/Q592, and Y11/Y597). The main differences in interactions are the contacts with S581 and R582 with Y11 that were not found in the docked complex. In



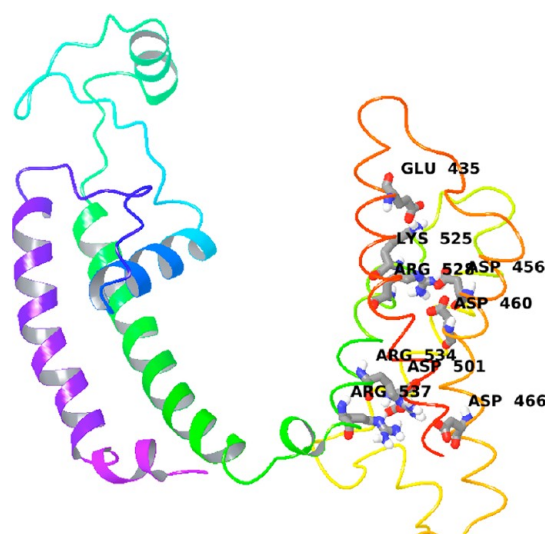


**Figure 3.** Salt bridge interactions at the voltage sensing domains of open state conformations (model 732) of the derived hERG1 model.

**Table 2. Docking Results of hERG1 Open-Inactivated State Homology Models from Glide/IFD Program**

model no.	docking for selective inactive state blockers				
	changrolin (pIC <sub>50</sub> , 4.74)		haloperidol (pIC <sub>50</sub> , 5.72)		H bonds with S631
	IFD score (kcal/mol)	Glide XP (kcal/mol)	IFD score (kcal/mol)	Glide XP (kcal/mol)	
88	-735.78	-4.01	-731.37	-4.23	–
227	-686.84	-1.96	-686.42	-4.04	–
355	-731.85	-5.74	-723.73	-5.61	–
380	-728.39	-3.51	-727.16	-6.88	–
453	-711.31	-6.21	-705.10	-5.08	–
634	-733.66	-5.80	-726.84	-5.36	–
710	-712.65	-5.06	-703.16	-4.57	–
1020	-737.82	-7.67	-734.57	-6.12	+
1325	-721.30	-3.04	-711.97	-1.05	–
1426	-735.21	-4.37	-732.25	-6.24	–
1548	-724.90	-2.58	-719.67	-2.09	+
1607	-731.90	-2.20	-726.06	0.00	–
1540	-705.94	-6.88	-700.15	0.00	–
1943	-625.44	-4.93	-610.50	-5.37	–
1979	-710.58	-3.83	-712.23	-7.21	+
1946	-679.97	-7.26	-646.23	-4.03	+

addition, Q592 not only forms an interaction with R20 but also interacts with D4, a contact which is not reported by Tseng et al.<sup>20</sup>

Similar to open and inactivated states, selected models were merged with an explicit membrane environment and prepared for all-atom MD simulations for testing their stabilities and further analysis. A 7.5 ns MD simulation has been performed for each model. Figure 2(iii) shows the RMSF values for the closed state model (851). The model has relatively large fluctuations at IC and EC linkers (<3.5 Å). While S5-pore linker has an RMSF value of 2.5–3.5 Å, the corresponding value of other domains is 1.5–2.0 Å throughout the simulations. Top (from EC site) and side views of a representative constructed closed state model (851) are shown at Figure 5.

**iv. Gating Charge Calculations.** The VSD of hERG1 is connected by S4S5 linker and has been found that it interacts

with PAS domain to regulate gating. It is thought to be an essential component of the activation gate for hERG channels. S4S5 linker is parallel to the cell membrane and interacts with the C-terminal residues at the S6 helix. In particular, the interaction between residue D540 at S4S5 linker with S6 segments effects the gating mechanism of the hERG1 channel. Recent studies showed that S4S5 linker may also interact with the N-terminal domain of the hERG1.<sup>41</sup> They show a switch-like response to membrane potential resulting from movement of positively charged residues (i.e., Arg or Lys) in the membrane field.<sup>42</sup> The S4-helix of the hERG1 model contains four positively charged residues which pair with negatively charged residues located in the S1–S3 domains stabilizing open and closed states of the channel. The charge distribution on the helix affects the transfer of gating charges. The charge transferred is the product of the magnitude of the moving charges times the fraction of the field it moves.<sup>43,44</sup>

The closed to open state conformational transition in hERG1 transfers a total of ~8 e<sup>–</sup>, whereas transition from open to open-inactivated state transfers a total of ~0.7 e<sup>–</sup> in the hERG1 channel.<sup>45</sup> Since derived open-inactivated state models do not involve VSD part, gating charge calculations have been performed only for closed to open state transitions. Average gating charge for closed/open states from the last 5 ns MD simulations has been found to be 7.64 e<sup>–</sup>, which is in good agreement with the experimental finding of 8 e<sup>–</sup> (Supporting Information, Figure S9).

## DISCUSSION

In the absence of the crystal structure of the hERG1 channel, investigation of a detailed channel structure and understanding of its atomistic determinants for hERG1 blockers and activators are of great interest at both the academic and the industrial levels. Better understanding of molecular mechanisms of hERG1/ligand interactions requires construction of validated protein models of the channel. Thus, homology models of hERG1 based on the available crystal structures of KcsA, Kv1.2, and KvAP have been generated (most of them do not involve VSD) by several research groups recently to address these challenges.<sup>3,20,46–48</sup> In the present study, protein-engineering studies combining different modeling techniques (homology modeling, de novo design, and all-atom MD simulations) are performed for derivation of three different states (i.e., closed, open, and open-inactivated) of the hERG1 channel. The constraint-driven de novo modeling assisted for modeling of missing parts at the template structure. A new development in ROSETTA allowed us to include distance and relative-angle constraints to dynamical sample conformation, and it was extensively tested recently for studies of K channels.<sup>49</sup>

**State-Dependent Drug Binding to hERG1. i. Interaction of hERG1 Channel Blockers with Pore Domain.** In cardiac myocytes development of delayed rectification and repolarization by K channels may lead to two different effects: it either activates slowly (I<sub>Ks</sub>) or much more rapidly (I<sub>Kr</sub>) and shows strong time-dependent rectification.<sup>50</sup> Expression of hERG leads in a channel with distinctive characteristics similar to those observed native in I<sub>Kr</sub>; thus, it is believed to have the hERG as its molecular basis.<sup>50</sup> hERG and I<sub>Kr</sub> are blocked by small organic molecules (i.e., dofetilide, E4031) which include methanesulfonanilide fragments. The molecular determinants for high-binding affinity of methanesulfonanilides include two aromatic residues (F656 and Y652) at the central cavity of hERG1 and residues on the pore helices that face into the

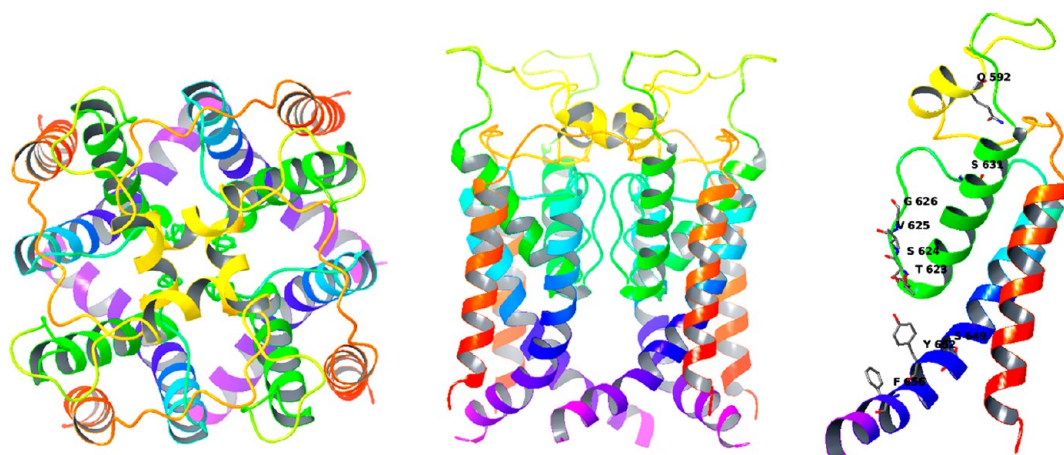


**Figure 4.** Representation of open-inactivated state model 1020 after MD simulations. (Left) Top view from EC; (mid) side view; (right) essential amino acids at PD of hERG channel blockers (for clarity, only one chain of the channel has been shown).

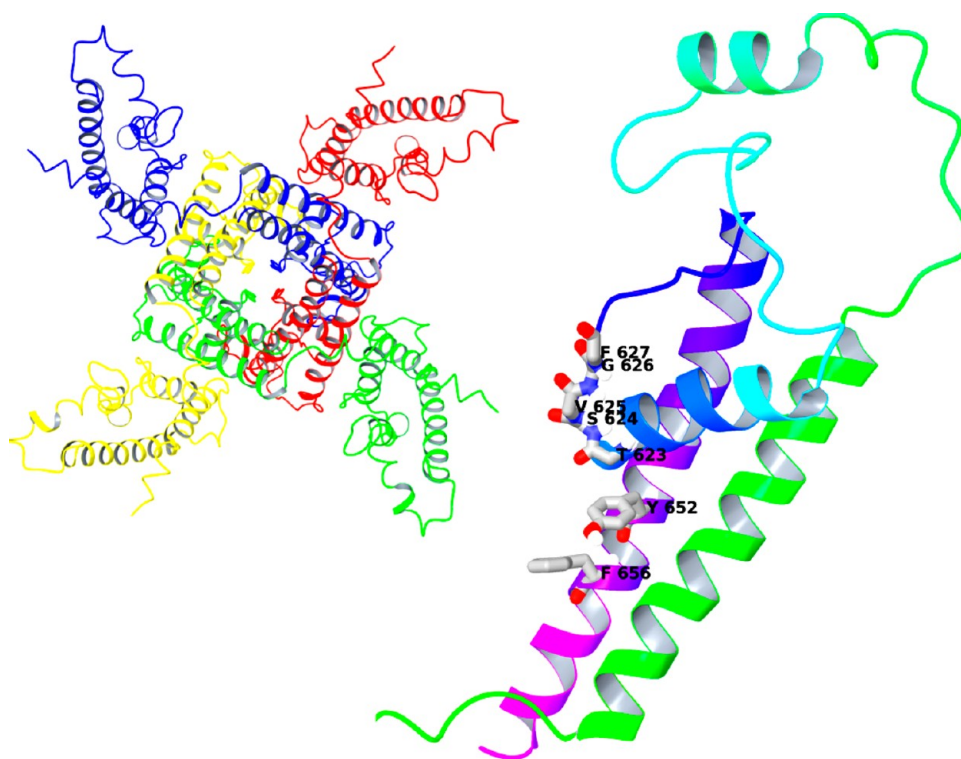


**Figure 5.** Representation of closed state model 851 after MD simulations. (Left) Top view from EC; (right) essential amino acids at PD of hERG channel blockers side view (for clarity, only one chain of the channel has been shown).

central cavity. Lees-Miller et al.<sup>36</sup> postulated that  $\pi$ -stacking interactions between aromatic groups of blockers and aromatic residues at the central cavity of the channel (i.e., F656 and Y652) of hERG1 are important for high-affinity blockade. Most of the high-affinity hERG1 blockers also include basic tertiary nitrogen (i.e., MK-499, cisapride, terfenadine), and a cation– $\pi$  interaction (with Y652) for these blockers is suggested by several research groups.<sup>51</sup> On the other hand, key residues for low-affinity blockers may be different.<sup>52</sup> Witchel et al.<sup>52</sup> reported that propafenone blocks the hERG1 channel in the open state, and its binding affinity ( $\text{pIC}_{50}$  5.64) is lower than that of methanesulfonanilides. They found that blockade of propafenone is strongly dependent on mutation of F656 but was insensitive to mutations of T623, S624, V625, G648, Y652, and V659.<sup>52</sup> When the hERG channel is in the closed state,

blockers are not able to bind to the channel; thus, opening of the activation gate is necessary.<sup>36</sup>

hERG currents display pronounced inward rectification due to rapid C-type inactivation, and it is essential for proper physiological functions underlying antiarrhythmic properties of the channel.<sup>53</sup> After hERG channel activation upon membrane potential depolarization, the channel rapidly (i.e., with a time constant of 12 ms at  $-20$  mV) shifts into an inactivated state to prevent  $\text{K}^+$  efflux.<sup>54</sup> The high-affinity blockers binding to hERG1 are known to either shift C-type inactivation or lock channels in their inactivated states. Several point mutations around the selectivity filter, pore helix, or outer mouth of the selectivity filter (i.e., S620T, N629D, S631C) may alter or even abolish the inactivation properties of hERG. Although a large number of mutations affecting inactivation in hERGs have been



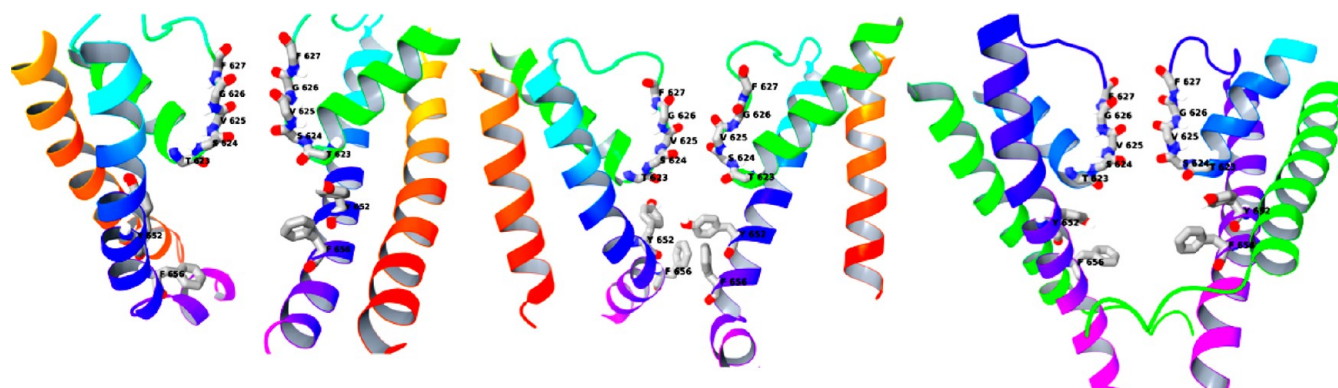


**Figure 6.** Comparison of central cavity residues F656 and Y652 and selectivity filter for open state (model 732) (left), open-inactivated state (model 1020) (mid), and closed state (model-851) (right) after MD simulations (for clarity, only two chains of the channel have been shown, side chains of selectivity filter residues are not shown.).

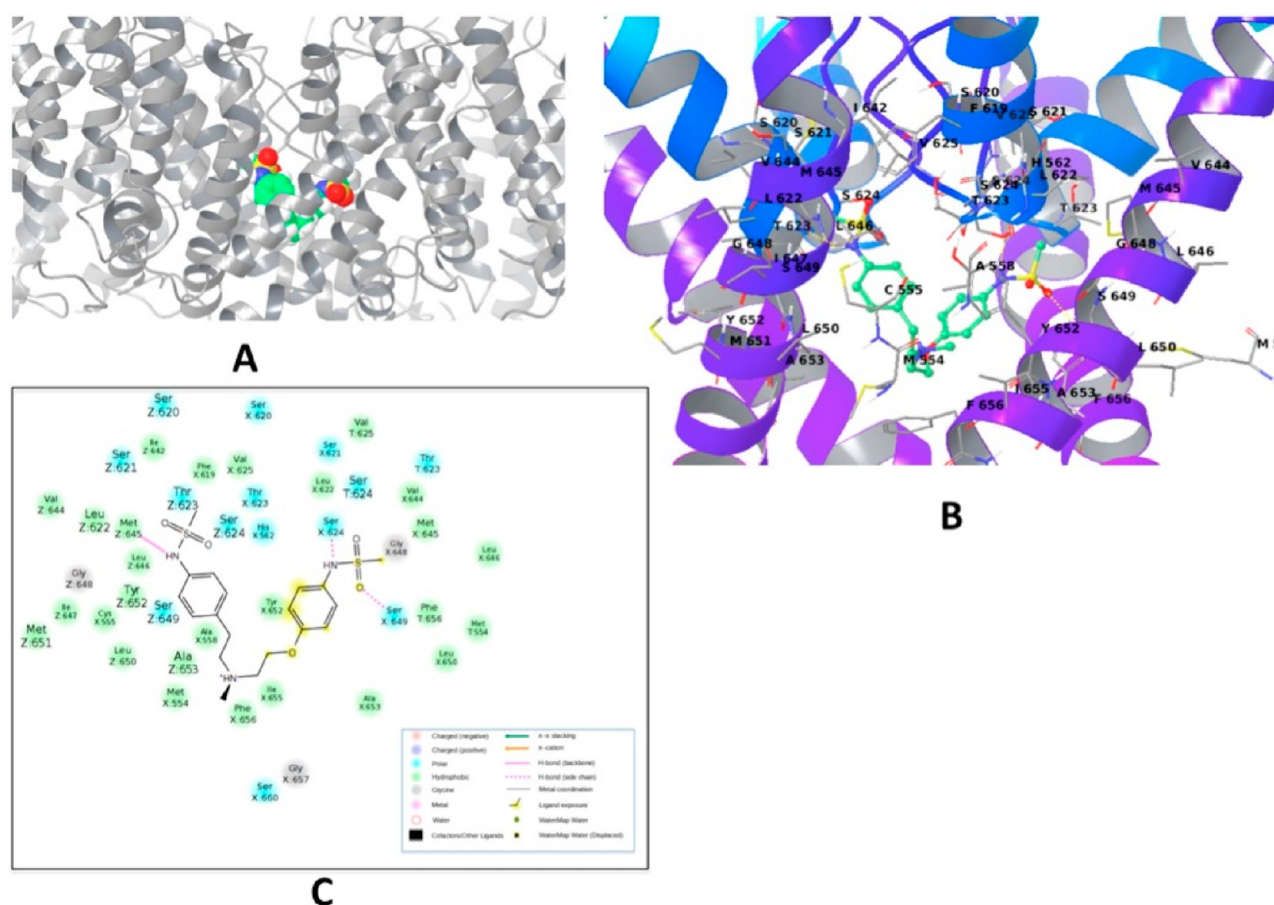


**Figure 7.** (A) Top docking pose of dofetilide at the central cavity of open state hERG1 structure. (B and C) 3D and 2D ligand interactions binding interactions, respectively.

reported, a structural understanding of rapid C-type inactivation in hERGs has only recently begun to emerge. Despite the structural similarities, there are important differences in the kinetics and voltage dependence of C-type inactivation between hERG and Shaker channels. In the hERG, the onset and reversal of C-type inactivation is very rapid and occur simultaneously with activation and deactivation of the channel, respectively.<sup>55</sup> C-type inactivation in Shaker channels is considerably slower and occurs only after the activation or deactivation process.<sup>55</sup>

Many of the drugs are targeting the C-type inactivated state of the channel, a feature that is widely believed to be involved into pro-arrhythmic properties of the drug-like molecule. How does this state-dependent blockade emerge? To answer this question we chose a set of state-specific hERG1 blockers. The state-selective hERG1 blockers (small organic molecules as well as toxin (BeKm-1)) are used for validating the constructed hERG1 models in our study. These compounds are docked to the SSS6 PD of hERG1 models since the architecture of the models differs in the putative opening and closing of the S6 helix between different states. Antiarrhythmic drugs identified

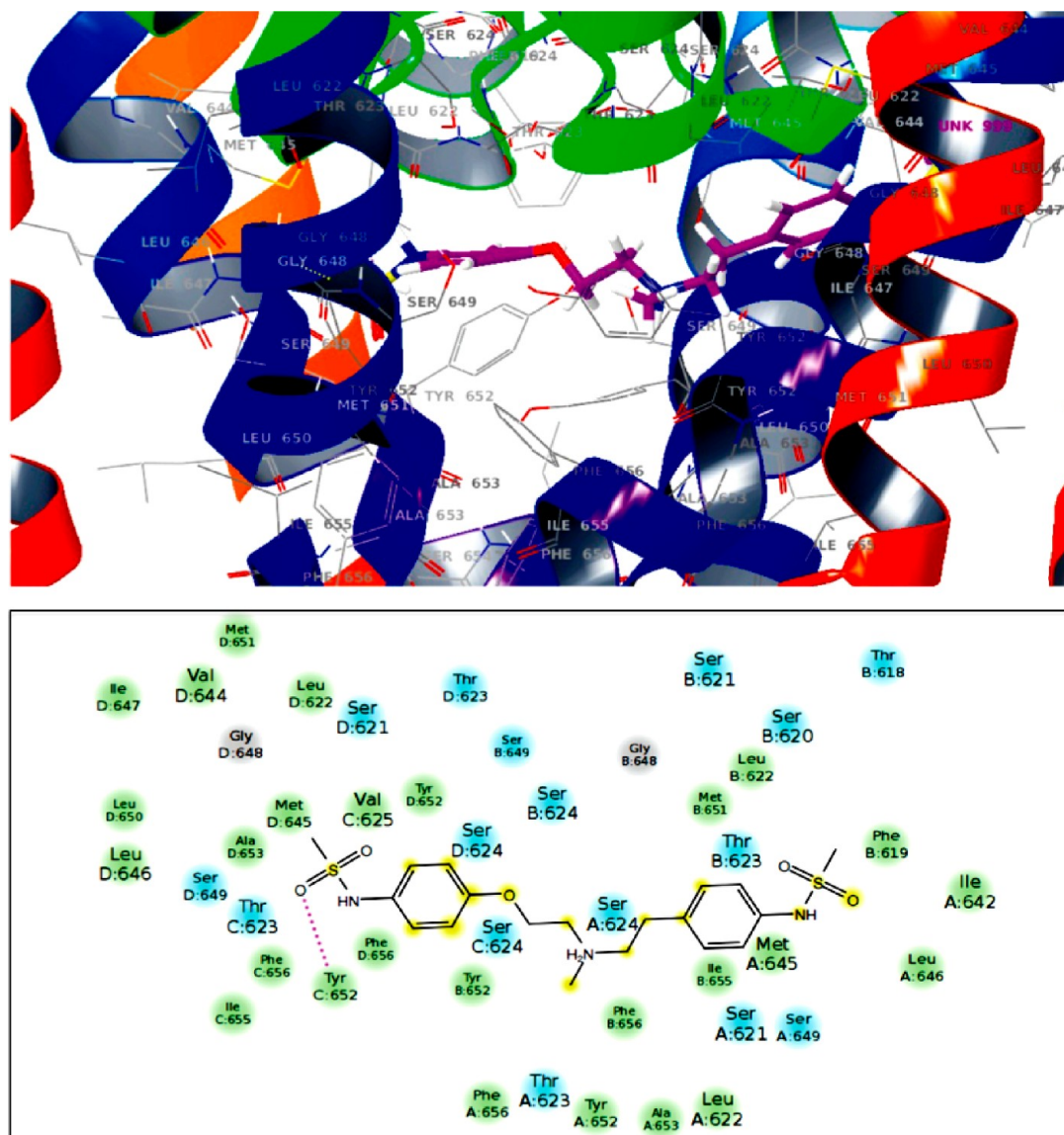


**Figure 8.** (Top) Docking pose of dofetilide, the central cavity of the open-inactivated state model. (Bottom) Corresponding 2D ligand interaction diagram.

from site-directed mutagenesis (SDM) experiments show state-selective binding to the hERG1 channel in the pore domain at different concentrations.<sup>36</sup> Since an ensemble of drug candidates has been found to block the channel in open and inactivated states with variable inhibition concentration and binding affinity, creation of successful hERG1 models by ligand docking testing using different blockers has become an essential validation technique.

We tested five different hERG1 blockers with diverse  $\text{pIC}_{50}$  values in binding to IC cavity. The idea of using diverse blockers (in terms of hERG1 blocking affinities) is to test the ligand/residue binding interactions with constructed homology models and to check their ability to distinguish weak, moderate, and strong affinity blockers. Certain hERG1 blockers including haloperidol and changrolin bind to the outer mouth of the channel (i.e., S631 site) and increase the degree and rate of inactivation in hERG1.<sup>37</sup> However, mutation of the channel (i.e., S631A) has been found to abolish inactivation gating, which also weakens haloperidol binding compared to wild-type channel.<sup>37</sup> Binding of haloperidol shows putative H bonding to

S631 in some of the inactivated state models (i.e., models 1020 and 1979 have been selected for future refinement tests).

Since many of the mutations at the pore domain in hERG (N629D in particular) and KcsA considerably alter the pore permeation and may potentially affect drug binding affinity through a gating-independent mechanism, conformational differences of different states in this region (N629) have also been checked. Comparison of conformations from the outer mouth of the selectivity filter shows different conformations of N629 at the three different states (Supporting Information, Figure S8).

It was proposed that the conformational dynamics of the distal S6 and the pore helix might be responsible for enhancement of the binding by C-type inactivation. A comparison of the conformations of central cavity residues which are essential for high-affinity drug blockade (i.e., F656 and Y652) and selectivity filter amino acids for three different states is shown in Figure 6. In order to further test derived open and open-inactivated state models, docking poses of well-known hERG1 blocker dofetilide at these targets have also been



analyzed. Dofetilide binding poses at the central cavity of hERG1 models showed that derived open and open-inactivated states are able to reproduce established specific target/ligand binding interactions (Figures 7 and 8). Amino-acid residues in the central cavity forming receptor site involve aromatic residues (Y652 and F656) and residues at the pore helix that face into the central cavity (i.e., T623, S624, M645, S649) in both the open and the open-inactivated state models. The main difference between binding to the open and the C-type inactivated state, however, is the conformation of the bound dofetilide. In contrast to the linear-like conformation at the open-inactivated state, the top-docking pose at the open state has a more compact form. This leads to a different fragment of dofetilide/residue interactions in two states. The linear-like conformation in dofetilide docking pose leads to close interactions with the residues in the nearby S4S5 IC site (i.e., F619, M645, L646). Furthermore, Y652 forms a H bond in the inactivated state together with hydrophobic interactions; however, this H bonding from the Y652 site does not exist in the open state model (Figures 7 and 8). Hydrogen bonds are observed between S624, S649, and M645 (backbone) and ligand at the open state model (Figure 7). The mechanism that underlies preferential binding to the inactivated states of some of hERG1 blockers is still under debate in several research groups. The change of conformation of the side chain of residues at the base of the pore helix during inactivation may facilitate drug binding.<sup>56</sup> Chen et al.<sup>57</sup> showed that repositioning of aromatic residues (Y652 and F656) at the S6 helix improved cisapride (an hERG blocker) binding independent of inactivation. The authors suggested that positioning of S6 aromatic residues relative to the central cavity of the channel and not the inactivation process determines cisapride blockade. However, repositioning of aromatic residues did not improve the blocking ability of another hERG blocker MK-499. This can be explained with different binding interactions of MK-499 and cisapride at the central cavity of the channel. Unlike cisapride, interactions of residues located at the base of the pore helix (i.e., T623, S624) can be important for MK-499 binding.

*ii. Proposed Mechanism of hERG1 Channel Activation and Inactivation.* Activation of the hERG1 channel from the closed to the open state transition measured using the Poisson–Boltzmann equation is in good agreement with experimental estimates of  $\sim 8 e^-$  (Supporting Information Figure S9). The magnitude of total gating charge transfer between open and closed states explains the strong coupling between the channel conformation and the applied membrane potential. This is contributed by four positively charged residues K525, R528, R531, and R534 in the S4 helix (Supporting Information Figure S10). Movement of S4 couples the bending of the S6 helix, thereby closing the pore in the closed state.<sup>58</sup> Gating charges calculated for the Kv1.2 channel<sup>29</sup> were found to be  $\sim 12 e^-$ , which is greater than the hERG1 channel by  $4-5 e^-$ . The difference between the gating charges for the two channels comes from the number of positively charged residues in the S4 helix. hERG1 contains one less positively charged residue than that of Shaker in the S4 helix. In addition, hERG1 has three extra negative charges in the S1, S2, and S3 helices. The presence of these negatively charged residues allows formation of strong salt-bridge contacts with the positively charged residues in the S4 helix, which stabilizes the open and closed states of the hERG1 channel and slows activation gating kinetics.<sup>45</sup> Our results clearly demonstrate the presence of these salt-bridge interactions in open and closed states. Salt-bridge

interaction analysis during MD simulations suggests that intrasubunit distances for charged residues in VSD of the open state model fluctuate between 2 and 4 Å, which signifies strong electrostatic interactions and correlates with experimental measurements (Figure 2). During the gating transition from the closed to the open state and stabilization of the open and closed states by salt-bridge formation, S4 has been found to undergo  $\sim 6-7$  Å movement along the  $z$  axis of the membrane normal (Supporting Information, Figure S10). S4 is the only voltage sensor domain for gating in Kv channels, and the coupling between the S4 movements and a conformational change in the outer mouth of selectivity filter region is very efficient in hERG compared to other Kv channels. The shift of S4 induces conformational change in the PD which is communicated by S4–S5 linker, and this causes tilting of the S6 hinge IFG motif (residues 655–657) to open and close the pore which involves  $\sim 8$  Å movements. Gayen et al.<sup>59</sup> recently investigated structural features of the S4S5 linker using circular dichroism (CD) and nuclear magnetic resonance (NMR). They found that the S4S5 linker had no well-ordered structure in aqueous solution and adopted a  $3_{10}$ -helix structure in DPC micelles. The structure predicted in DPC micelles can be considered close to the physiological structure of the linker because it is very close to the cell membrane. In their proposed S4S5 linker structure (in micelles), D540 faced the solution and displayed the structural basis for construction of salt-bridge interactions with adjacent positively charged residues. A short helix at the S4S5 linker part (residues 540–543) was also observed in our open state models (i.e., model 732) representing the consistency between modeling and the NMR-based defined structure (Supporting Information, Figure S11). Parallel to the experimental study, in our models D540 faces the solution and has close contacts with adjacent positively charged residues. For example, in the closed state a salt-bridge interaction is formed (between D540 and R665) to stabilize the closed state of the channel. Sanguinetti and Xu<sup>60</sup> studied another mutation in the S4S5 linker part (E544A), and they reported that this mutation activated faster than the wild-type channel, whereas mutation of E544K activated the hERG1 channel slower compared to wild type. E544A mutation might change its interaction with positively charged residue R541, and it may lead to change the channel activation rate. However, the mutation to positive charged residue (E544K) may lead to repulsion between E544K and R541 so may lead to a slower activation rate.<sup>59</sup> Parallel to experimental findings a close contact between R541 and E544 has been formed in our model structures. Close-contact distances between residues R541 and E544 at the closed state are shorter than the open state in our structures (Supporting Information, Figure S12).

The rapid conformational dynamics in the region of the outer mouth of the selectivity filter domain was proposed to be a key driver for fast C-type inactivation in hERG channels. Conformational transition between the open and the inactivated state occurs on time scales of 10–20 ms.<sup>37</sup> It is yet to be established of how rearrangements in this region are coupled to the dynamics of the voltage sensor. It was proposed that in Shaker channels, where C-type inactivation is slow, the conformational changes in the outer mouth of the channel are lagging behind the S4 movements involved in the channel's activation.<sup>55</sup> It could be a long-distance coupling between the dynamics of the voltage-sensor and the outer-mouth region in hERG1 that makes it inactivate faster. The first attempt at modeling the inactivated state in hERG using the published



KcsA structure was made by Stansfield et al.<sup>54</sup> in 2008. In that study it was shown that the carbonyl group of the aromatic residue (F627) at the selectivity filter rotates away from the conduction axis in wild-type channel; however, in mutant channels this conformational change occurs rarely. In non-inactivated channels, interactions with water molecules occupying the behind the selectivity filter are playing an important role in enhancing the stability of the conducting state. This observation is confirmed by recent NMR studies of KcsA gating dynamics.<sup>61</sup> Our derived models may provide further insights into mechanisms of C-type inactivation of hERG1 channel. First, the conformation of the selectivity filter observed for the open-inactivated state differs from that observed in open and closed states. The backbone carbonyl oxygens lining the permeation pathway are flipping away (Figure 6), thus leading to a collapsed conformation of the selectivity filter. Movement of S6 helices observed in inactivated models primarily mediates collapse of the filter. Movement of the putative glycine hinge IFG motif (residues 655–657) in S6 causes further widening of the pore as compared to the open state model. Computational studies on KcsA in the inactivated state suggest that widening of the pore causes a decrease in  $\psi$  angle measured between the  $z$  axis and the cytoplasmic end of S6 helix axis.<sup>6</sup> We analyzed the plane angle ( $\psi$ ) (defined between the  $z$  axis and the core axis of the C-terminal half of TM6) during the MD simulations of hERG1 models. Values from the last 5 ns MD simulations from each state were used for analysis (Supporting Information, Figure S13). Our inactivated state models display these large S6 movements and conformational change of the filter, which confirms the hypothesis stated above.

Figure 9 shows the superimposition of open, open-inactivated, and closed states of derived hERG1 models.

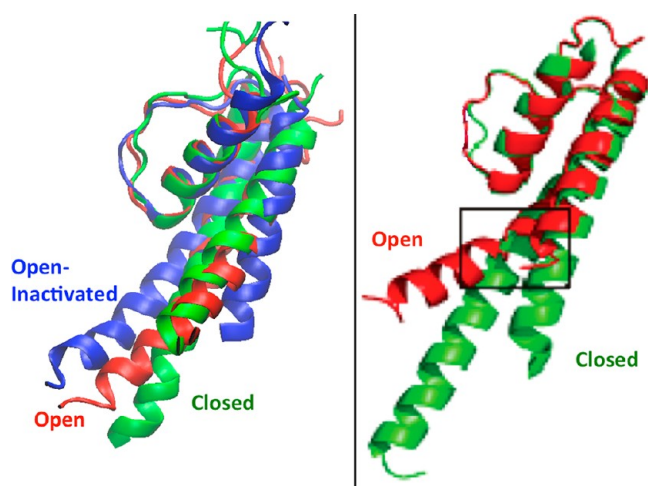


**Figure 9.** (Left) Superimposition of pore domains of open (red), open-inactivated (blue), and closed states (green) of hERG1 models. (Right) Reported open and closed states of KcsA conformations by Cuello et al.<sup>6</sup>

Hinge-bending motion and rotation of the C-terminal half of TM6 leads to different conformations at the intracellular face of pore domains for three different states. The backbone hydrogen-bond distances ( $i$ ,  $i+4$ ) for the TM6 (residue numbers 643–664) are calculated for open, open-inactivated, and closed states of hERG1 (distances are average values from the last 5000 frames of MD simulations from each state)

(Supporting Information, Figure S14). An increase in backbone H-bond distance leads a break in intra-helix H bonds and obtained results show similarities with the Cuello et al.<sup>6</sup> study on the KcsA channel. Apart from these changes, the inactivated models also predict the spatial proximity of S5 (W568 to T618) in the pore helix. It was reported recently that mutations of the S5 residues in close proximity to T618 abolishes inactivation gating.<sup>62</sup> The spatial proximity of the S5-pore helix and conformational coupling of selectivity filter-S6 suggests unique conformational rearrangements revealed by a model of inactivated hERG1 PD (Supporting Information, Figure S15).  $C_{\alpha}$ – $C_{\alpha}$  distances between W568 and T618 are compared for three states, and average distances are found to be 11.3, 9.9, and 6.4 Å for closed, open, and open-inactivated states, respectively. (Supporting Information, Figure S15).

**iii. Implications for Novel Drug Design.** Creation of hERG1 channel models in three different states is not only important for better understanding of the hERG1 blockers mechanism but also is important for hERG1 activators. Activators of channels are promising candidates to restore channel function in acquired or inherited channelopathies. The mandatory screening of novel drug candidates for hERG1 activity has resulted in recent reports of some compounds that enhance the hERG current. However, knowledge is quite limited about their structural mechanism of action. It is known that hERG1 channel openers are not uniform in their biophysical mechanism of action. Some drugs increase hERG currents by shifting the voltage dependence of C-type inactivation to more depolarizing potentials, whereas some shift the  $V_{0.5}$  of voltage-dependent activation to more hyperpolarized potentials or slow the kinetics of deactivation (stabilizing the open state of the channel). Some familial mutations in hERG1 result in channels with voltage-dependent inactivation thresholds shifted substantially to the right (depolarized potentials). This shift can result in an increase in the time-dependent current at the expense of a decrease in the antiarrhythmic tail current. These mutations can lead to familial short-QT Syndrome (SQTS). In contrast, drugs that increase the magnitude of the tail current or slow its deactivation can be antiarrhythmic. Recent reports of Schuster et al.<sup>64</sup> and Gerlach et al.<sup>65</sup> state that novel channel openers (i.e., NS1643, ICA-105574) may display selective binding to a certain conformation of hERG1. Thus, better understanding of their conformation-dependent mechanism controlling drug stabilization opens new avenues for rational design of novel compounds targeting hERGs.

## CONCLUSIONS

In summary, our study reports on the structural models of the hERG1 K channel in different conformations. The hERG1 channel is homologous to other Kv channels but possesses low sequence identity. To circumvent limitations of standard homology modeling techniques we used de novo ROSETTA modeling with incorporated experimental constraints. Several state-selective blockers were docked to models of open and inactivated states of hERG1 using the Glide/IFD method. The complex for hERG1/BeKm-1 toxin was obtained using the HADDOCK protein/protein docking algorithm for validation of the closed state models. The set of homology models incorporating multiple experimental constraints (salt bridges, close contacts, helix angles, and accessibility) was found to provide good correlation with experimental  $pIC_{50}$  values for high- and low-affinity blockers. Computation of gating charges are further validated in our closed and open state models.

Derived models of hERG1 in different states offer an indispensable template for rational drug design as well as better understanding of the molecular mechanisms of the hERG1 channel upon binding of openers or blockers. Derived homology models are freely available upon request.

## ■ ASSOCIATED CONTENT

### ■ Supporting Information

Alignment used for homology models, homology modeling scheme used for building hERG1 structures, bond length and bond angle deviations for the derived models, Ramachandran plots for selected models, salt-bridge interactions observed between positive charged residues in S4 helix and negative charged residues in S1–S3 helices of open state model 732 during MD simulations, top docking pose of haloperidol at the open-inactivated state, interactions of BeKm-1 toxin at the closed state model, superimposition of channels at the region of N629, gating charge calculations of open/closed state models, superimposition of hERG1 open state and closed states, center of mass shift differences of positive charged residues (gating residues) at S4 helix of closed and open state channels throughout the MD simulations, S4S5 linker part for derived open state models, distance between the side chains of E544 and R541 for open and closed state models throughout MD simulations, plane angle change during MD simulations of hERG1 models, backbone H-bond distance for the TM6 (643–664) for closed, open, and open-inactivated states, locations of T618 and W568 residues at the constructed inactivated state hERG1 homology model, change of  $\alpha$ – $\alpha$  distances at T618–W568 during MD simulations of open, open-inactivated, and closed states of hERG1, salt-bridge contacts at the derived initial (nonrefined) open state hERG1 models, rmsd and alignment scores for hERG1 models, docking results of hERG1 closed state homology models from HADDOCK protein/protein docking program. This material is available free of charge via the Internet at <http://pubs.acs.org>.

## ■ AUTHOR INFORMATION

### Corresponding Author

\*Tel.: (+1) 403-7971. Fax: (+1) 403-210-8655. E-mail: [snoskov@ucalgary.ca](mailto:snoskov@ucalgary.ca) (S.Y.N.); [hduff@ucalgary.ca](mailto:hduff@ucalgary.ca) (H.J.D.).

### Notes

The authors declare no competing financial interest.

## ■ ACKNOWLEDGMENTS

This work was supported by the Canadian Institutes of Health Research-CIHR (MOP-186232) to S.N. and H.J.D. and the Heart and Stroke Foundation of Alberta (H.J.D. and S.N.). S.N. is CIHR New Investigator and an Alberta Heritage Foundation for Medical Research (AHFMR) Scholar. Research of S.D. is supported by CIHR and Alberta Innovates Health Solutions (AIHS) PDF awards. H.J.D. is an AHFMR Medical Scientist. Computational support for this work was provided by the West-Grid Canada through a resource allocation award to S.N.

## ■ REFERENCES

- (1) Durdagi, S.; Subbotina, J.; Lees-Miller, J.; Guo, J.; Duff, H. J.; Noskov, S. Y. Insights into the molecular mechanism of hERG1 channel activation and blockade by drugs. *Curr. Med. Chem.* **2010**, *17* (30), 3514–32.
- (2) Suessbrich, H.; Schonherr, R.; Heinemann, S. H.; Lang, F.; Busch, A. E. Specific block of cloned Herg channels by clofilium and its tertiary analog LY97241. *FEBS Lett.* **1997**, *414* (2), 435–8.

- (3) Subbotina, J.; Yarov-Yarovoy, V.; Lees-Miller, J.; Durdagi, S.; Guo, J.; Duff, H. J.; Noskov, S. Y. Structural refinement of the hERG1 pore and voltage-sensing domains with ROSETTA-membrane and molecular dynamics simulations. *Proteins* **2010**, *78* (14), 2922–34.

- (4) Yarov-Yarovoy, V.; Baker, D.; Catterall, W. A. Voltage sensor conformations in the open and closed states in ROSETTA structural models of K(+) channels. *Proc. Natl. Acad. Sci. U.S.A.* **2006**, *103* (19), 7292–7.

- (5) Cuello, L. G.; Jogini, V.; Cortes, D. M.; Pan, A. C.; Gagnon, D. G.; Dalmas, O.; Cordero-Morales, J. F.; Chakrapani, S.; Roux, B.; Perozo, E. Structural basis for the coupling between activation and inactivation gates in K(+) channels. *Nature* **2010**, *466* (7303), 272–5.

- (6) Cuello, L. G.; Jogini, V.; Cortes, D. M.; Perozo, E. Structural mechanism of C-type inactivation in K(+) channels. *Nature* **2010**, *466* (7303), 203–8.

- (7) Thompson, J. D.; Higgins, D. G.; Gibson, T. J. Clustal-W - Improving the Sensitivity of Progressive Multiple Sequence Alignment through Sequence Weighting, Position-Specific Gap Penalties and Weight Matrix Choice. *Nucleic Acids Res.* **1994**, *22* (22), 4673–4680.

- (8) Raman, S.; Vernon, R.; Thompson, J.; Tyka, M.; Sadreyev, R.; Pei, J. M.; Kim, D.; Kellogg, E.; DiMaio, F.; Lange, O.; Kinch, L.; Sheffler, W.; Kim, B. H.; Das, R.; Grishin, N. V.; Baker, D. Structure prediction for CASP8 with all-atom refinement using Rosetta. *Proteins* **2009**, *77*, 89–99.

- (9) Chivian, D.; Baker, D. Homology modeling using parametric alignment ensemble generation with consensus and energy-based model selection. *Nucleic Acids Res.* **2006**, *34*, 17.

- (10) Chivian, D.; Baker, D. Homology modeling using parametric alignment ensemble generation with consensus and energy-based model selection. *Nucleic Acids Res.* **2006**, *34* (17), e112.

- (11) Wang, C.; Bradley, P.; Baker, D. Protein-protein docking with backbone flexibility. *J. Mol. Biol.* **2007**, *373* (2), 503–519.

- (12) Canutescu, A. A.; Dunbrack, R. L. Cyclic coordinate descent: A robotics algorithm for protein loop closure. *Protein Sci.* **2003**, *12* (5), 963–972.

- (13) Subbotina, J.; Yarov-Yarovoy, V.; Lees-Miller, J.; Durdagi, S.; Guo, J. Q.; Duff, H. J.; Noskov, S. Y. Structural refinement of the hERG1 pore and voltage-sensing domains with ROSETTA-membrane and molecular dynamics simulations. *Proteins* **2010**, *78* (14), 2922–2934.

- (14) Long, S. B.; Campbell, E. B.; MacKinnon, R. Crystal structure of a mammalian voltage-dependent Shaker family K<sup>+</sup> channel. *Science* **2005**, *309* (5736), 897–903.

- (15) Yarov-Yarovoy, V.; Baker, D.; Catterall, W. A. Voltage sensor conformations in the open and closed states in ROSETTA structural models of K<sup>+</sup> channels. *Proc. Natl. Acad. Sci. U.S.A.* **2006**, *103* (19), 7292–7297.

- (16) McGuffin, L. J.; Bryson, K.; Jones, D. T. The PSIPRED protein structure prediction server. *Bioinformatics* **2000**, *16* (4), 404–405.

- (17) Abagyan, R.; Totrov, M.; Kuznetsov, D. Icm - a New Method for Protein Modeling and Design - Applications to Docking and Structure Prediction from the Distorted Native Conformation. *J. Comput. Chem.* **1994**, *15* (5), 488–506.

- (18) Zhang, M.; Liu, J.; Jiang, M.; Wu, D. M.; Sonawane, K.; Guy, H. R.; Tseng, G. N. Interactions between charged residues in the transmembrane segments of the voltage-sensing domain in the hERG channel. *J. Membr. Biol.* **2005**, *207* (3), 169–181.

- (19) Tristani-Firouzi, M.; Chen, J.; Sanguinetti, M. C. Interactions between S4-S5 linker and S6 transmembrane domain modulate gating of HERG K<sup>+</sup> channels. *J. Biol. Chem.* **2002**, *277* (21), 18994–19000.

- (20) Tseng, G. N.; Sonawane, K. D.; Korolkova, Y. V.; Zhang, M.; Liu, J.; Grishin, E. V.; Guy, H. R. Probing the outer mouth structure of the hERG channel with peptide toxin footprinting and molecular modeling. *Biophys. J.* **2007**, *92* (10), 3524–3540.

- (21) Schrodinger.

- (22) Sherman, W.; Day, T.; Jacobson, M. P.; Friesner, R. A.; Farid, R. Novel procedure for modeling ligand/receptor induced fit effects. *J. Med. Chem.* **2006**, *49* (2), 534–53.

- (23) Friesner, R. A.; Murphy, R. B.; Repasky, M. P.; Frye, L. L.; Greenwood, J. R.; Halgren, T. A.; Sanschagrin, P. C.; Mainz, D. T. Extra precision glide: docking and scoring incorporating a model of hydrophobic enclosure for protein-ligand complexes. *J. Med. Chem.* **2006**, *49* (21), 6177–96.
- (24) Jacobson, M. P.; Pincus, D. L.; Rapp, C. S.; Day, T. J.; Honig, B.; Shaw, D. E.; Friesner, R. A. A hierarchical approach to all-atom protein loop prediction. *Proteins* **2004**, *55* (2), 351–67.
- (25) Dominguez, C.; Boelens, R.; Bonvin, A. M. HADDOCK: a protein-protein docking approach based on biochemical or biophysical information. *J. Am. Chem. Soc.* **2003**, *125* (7), 1731–7.
- (26) Kumar, R.; Iyer, V. G.; Im, W. CHARMM-GUI: A graphical user interface for the CHARMM users. *Abstr. Pap. Am. Chem. Soc.* **2007**, *233*, 273–273.
- (27) Jo, S.; Kim, T.; Iyer, V. G.; Im, W. Software news and updates - CHARMM-GUI: A web-based graphical user interface for CHARMM. *J. Comput. Chem.* **2008**, *29* (11), 1859–1865.
- (28) Callenberg, K. M.; Choudhary, O. P.; de Forest, G. L.; Gohara, D. W.; Baker, N. A.; Grabe, M.; APBSmem: a graphical interface for electrostatic calculations at the membrane. *Plos One* **2010**, *5* (9).
- (29) Khalili-Araghi, F.; Jogini, V.; Yarov-Yarovoy, V.; Tajkhorshid, E.; Roux, B.; Schulten, K. Calculation of the gating charge for the Kv1.2 voltage-activated potassium channel. *Biophys. J.* **2010**, *98* (10), 2189–98.
- (30) Sharp, K. Calculating Electrostatic Forces in Molecular-Dynamics Using the Finite-Difference Poisson-Boltzmann Method. *Biophys. J.* **1990**, *57* (2), A10–A10.
- (31) Piper, D. R.; Rupp, J.; Sachse, F. B.; Sanguinetti, M. C.; Tristani-Firouzi, M. Cooperative interactions between R531 and acidic residues in the voltage sensing module of hERG1 channels. *Cell. Physiol. Biochem.* **2008**, *21* (1–3), 37–46.
- (32) Jiang, M.; Zhang, M.; Maslennikov, I. V.; Liu, J.; Wu, D. M.; Korolkova, Y. V.; Arseniev, A. S.; Grishin, E. V.; Tseng, G. N. Dynamic conformational changes of extracellular S5-P linkers in the hERG channel. *J. Physiol. London* **2005**, *569* (1), 75–89.
- (33) Subbiah, R. N.; Kondo, M.; Campbell, T. J.; Vandenberg, J. I. Tryptophan scanning mutagenesis of the HERG K<sup>+</sup> channel: the S4 domain is loosely packed and likely to be lipid exposed. *J. Physiol.* **2005**, *569* (Pt 2), 367–79.
- (34) Piper, D. R.; Rupp, J.; Sachse, F. B.; Sanguinetti, M. C.; Tristani-Firouzi, M. Cooperative interactions between R531 and acidic residues in the voltage sensing module of hERG1 channels. *Cell. Physiol. Biochem.: Int. J. Exp. Cell. Physiol., Biochem., Pharmacol.* **2008**, *21* (1–3), 37–46.
- (35) Subbiah, R. N.; Kondo, M.; Campbell, T. J.; Vandenberg, J. I. Tryptophan scanning mutagenesis of the HERG K<sup>+</sup> channel: the S4 domain is loosely packed and likely to be lipid exposed. *J. Physiol., London* **2005**, *569* (2), 367–379.
- (36) Lees-Miller, J. P.; Duan, Y.; Teng, G. Q.; Duff, H. J. Molecular determinant of high-affinity dofetilide binding to HERG1 expressed in *Xenopus* oocytes: involvement of S6 sites. *Mol. pharmacol.* **2000**, *57* (2), 367–74.
- (37) Suessbrich, H.; Schonherr, R.; Heinemann, S. H.; Attali, B.; Lang, F.; Busch, A. E. The inhibitory effect of the antipsychotic drug haloperidol on HERG potassium channels expressed in *Xenopus* oocytes. *Br. J. Pharmacol.* **1997**, *120* (5), 968–74.
- (38) Jogini, V.; Roux, B. Dynamics of the Kv1.2 voltage-gated K<sup>+</sup> channel in a membrane environment. *Biophys. J.* **2007**, *93* (9), 3070–82.
- (39) Durdagi, S.; Duff, H. J.; Noskov, S. Y. Combined receptor and ligand-based approach to the universal pharmacophore model development for studies of drug blockade to the hERG1 pore domain. *J. Chem. Inf. Model.* **2011**, *51* (2), 463–74.
- (40) Chen, W. H.; Wang, W. Y.; Zhang, J.; Yang, D.; Wang, Y. P. State-dependent blockade of human ether-a-go-go-related gene (hERG) K(+) channels by changrolin in stably transfected HEK293 cells. *Acta Pharmacol. Sin.* **2010**, *31* (8), 915–22.
- (41) Gustina, A. S.; Trudeau, M. C. A recombinant N-terminal domain fully restores deactivation gating in N-truncated and long QT syndrome mutant hERG potassium channels. *Proc. Natl. Acad. Sci. U.S.A.* **2009**, *106* (31), 13082–13087.
- (42) Tao, X.; Lee, A.; Limapichat, W.; Dougherty, D. A.; MacKinnon, R. A Gating Charge Transfer Center in Voltage Sensors. *Science* **2010**, *328* (5974), 67–73.
- (43) Cha, A.; Snyder, G. E.; Bezanilla, F., The voltage sensor in voltage-dependent ion channels. (vol 402, pg 809, 1999). *Physiol. Rev.* **2000**, *80* (3), U2–U2.
- (44) Bezanilla, F. How membrane proteins sense voltage. *Nat. Rev. Mol. Cell. Biol.* **2008**, *9* (4), 323–332.
- (45) Zhang, M.; Liu, J.; Tseng, G. N. Gating charges in the activation and inactivation processes of the hERG channel. *J. Gen. Physiol.* **2004**, *124* (6), 703–718.
- (46) Gepp, M. M.; Hutter, M. C. Determination of hERG channel blockers using a decision tree. *Bioorg. Med. Chem.* **2006**, *14* (15), 5325–5332.
- (47) Osterberg, F.; Aqvist, J. Exploring blocker binding to a homology model of the open hERG K<sup>+</sup> channel using docking and molecular dynamics methods. *FEBS Lett.* **2005**, *579* (13), 2939–2944.
- (48) Kuttah, R.; Vandenberg, J. I.; Kuyucak, S. Molecular dynamics and continuum electrostatics studies of inactivation in the HERG potassium channel. *J. Phys. Chem. B* **2007**, *111* (5), 1090–1098.
- (49) Catterall, W. A.; Yarov-Yarovoy, V. Helical motion of an S4 voltage sensor revealed by gating pore currents. *Channels (Austin)* **2010**, *4* (2), 75–7.
- (50) Wang, S.; Liu, S.; Morales, M. J.; Strauss, H. C.; Rasmusson, R. L. A quantitative analysis of the activation and inactivation kinetics of HERG expressed in *Xenopus* oocytes. *J. Physiol.* **1997**, *502* (Pt 1), 45–60.
- (51) Fernandez, D.; Ghanta, A.; Kauffman, G. W.; Sanguinetti, M. C. Physicochemical features of the hERG channel drug binding site. *J. Biol. Chem.* **2004**, *279* (11), 10120–10127.
- (52) Witchel, H. J.; Dempsey, C. E.; Sessions, R. B.; Perry, M.; Milnes, J. T.; Hancox, J. C.; Mitcheson, J. S. The low-potency, voltage-dependent HERG blocker propafenone - Molecular determinants and drug trapping. *Mol. Pharmacol.* **2004**, *66* (5), 1201–1212.
- (53) Stansfeld, P. J.; Sutcliffe, M. J.; Mitcheson, J. S. Molecular mechanisms for drug interactions with hERG that cause long QT syndrome. *Expert Opin. Drug Metab. Toxicol.* **2006**, *2* (1), 81–94.
- (54) Stansfeld, P. J.; Grottesi, A.; Sands, Z. A.; Sansom, M. S. P.; Gedeck, P.; Gosling, M.; Cox, B.; Stanfield, P. R.; Mitcheson, J. S.; Sutcliffe, M. J. Insight into the mechanism of inactivation and pH sensitivity in potassium channels from molecular dynamics simulations. *Biochemistry* **2008**, *47* (28), 7414–7422.
- (55) Fan, J. S.; Jiang, M.; Dun, W.; McDonald, T. V.; Tseng, G. N. Effects of outer mouth mutations on hERG channel function: A comparison with similar mutations in the Shaker channel. *Biophys. J.* **1999**, *76* (6), 3128–3140.
- (56) Wong, O. I.; Schawinski, K.; Kaviraj, S.; Masters, K. L.; Nichol, R. C.; Lintott, C.; Keel, W. C.; Darg, D.; Bamford, S. P.; Andreescu, D.; Murray, P.; Raddick, M. J.; Szalay, A.; Thomas, D.; Vandenberg, J. Galaxy Zoo: building the low-mass end of the red sequence with local post-starburst galaxies. *Mon. Not. R. Astron. Soc.* **2012**, *420* (2), 1684–1692.
- (57) Chen, J.; Seebohm, G.; Sanguinetti, M. C. Position of aromatic residues in the S6 domain, not inactivation, dictates cisapride sensitivity of HERG and eag potassium channels. *Proc. Natl. Acad. Sci. U.S.A.* **2002**, *99* (19), 12461–12466.
- (58) Schoppa, N. E.; McCormack, K.; Tanouye, M. A.; Sigworth, F. J. The size of gating charge in wild-type and mutant Shaker potassium channels. *Science* **1992**, *255* (5052), 1712–5.
- (59) Gayen, S.; Li, Q.; Kang, C. The solution structure of the S4-S5 linker of the hERG potassium channel. *J. Pept. Sci.* **2012**, *18* (2), 140–5.
- (60) Sanguinetti, M. C.; Xu, Q. P. Mutations of the S4-S5 linker alter activation properties of HERG potassium channels expressed in *Xenopus* oocytes. *J. Physiol., London* **1999**, *514* (3), 667–675.



- (61) Imai, S.; Osawa, M.; Takeuchi, K.; Shimada, I. Structural basis underlying the dual gate properties of KcsA. *Proc. Natl. Acad. Sci. U.S.A.* **2010**, *107* (14), 6216–6221.
- (62) Ferrer, T.; Cordero-Morales, J. F.; Arias, M.; Ficker, E.; Medovoy, D.; Perozo, E.; Tristani-Firouzi, M. Molecular coupling in the human ether-a-go-go-related gene-1 (hERG1) K<sup>+</sup> channel inactivation pathway. *J. Biol. Chem.* **2011**, *286* (45), 39091–9.
- (63) Kuttah, R.; Vandenberg, J. I.; Kuyucak, S. Molecular dynamics and continuum electrostatics studies of inactivation in the HERG potassium channel. *J. Phys. Chem. B* **2007**, *111* (5), 1090–8.
- (64) Schuster, A. M.; Glassmeier, G.; Bauer, C. K. Strong Activation of ether-a-go-go-Related Gene 1 K(+) Channel Isoforms by NS1643 in Human Embryonic Kidney 293 and Chinese Hamster Ovary Cells. *Mol. Pharmacol.* **2011**, *80* (5), 930–942.
- (65) Gerlach, A. C.; Stoehr, S. J.; Castle, N. A. Pharmacological Removal of Human Ether-a-go-go-Related Gene Potassium Channel Inactivation by 3-Nitro-N-(4-phenoxyphenyl) Benzamide (ICA-105574). *Mol. Pharmacol.* **2010**, *77* (1), 58–68.